Synthesis of 1,4,5,8,9,12-Hexabromododecahydrotriphenylene and Its

Application in Constructing Polycyclic Thioaromatics

Junfa Wei*, Xiaowei Jia, Jun Yu, Xianying Shi, Congjie Zhang, and Zhanguo Chen

School of Chemistry and Materials Science, Shaanxi Normal University, Xi'an, 710062, P. R. China

Fax:+86-029-85307774
E-mail: weijf@snnu.edu.cn

SUPPORTING INFORMATION:

Contents:

1. General Information.

Unless otherwise mentioned, all commercial reagents were used as received without further purification. The reactions were monitored using analytical thin layer chromatography (TLC) with Merck silica gel plate (GF-254). Flash chromatography was performed using Merck silica gel 60 with freshly distilled solvents. ^{1}H NMR (300 MHz) and ^{13}C NMR (75 MHz) spectra were recorded on Bruker Avance spectrometers using $CDCl_3$ as a solvent. Chemical shifts (δ) are reported in ppm, using TMS as an internal standard. Data are presented as follows: chemical shift (ppm), multiplicity (s = singlet, d = doublet, t = triplet, q = quartet, m = multiplet, b = broad), coupling constant J (Hz) and integration. Elemental analysis was performed on a PE-2400CHN (U.S) analyzer. Melting points were uncorrected. Infrared spectra were recorded using EQUINX55 FT-IR spectrometer (Brucher). The crystal structure was recorded on Bruker APEX II CCD area-detector X-ray diffraction spectrometer. Mass spectra data were obtained using a GCMS-QP2010nc Plus mass spectrometer (EI).

2. Experimental details and characterization of the compounds

Decahydrotriphenylene (6)

A mixture of cyclohexanone (1.16 mol, 120 mL) and zirconium tetrachloride (46.4 mmol, 10.8 g) in a 250 mL round-bottomed flask equipped with a condenser was allowed to stir under reflux for 10 h until the reaction mixture was solidified completely. The resultant solid product was dissolved in $CHCl_3$ and the catalyst was removed by filtration. The filtrate was concentrated under reduced pressure, and then EtOH was added into the residue. The precipitation was collected by filtration to give white powder in 71 % yield. The white powder was further purified by recrystallization with $CHCl_3$–EtOH. m.p.: 230.0-231.0 °C.
^{1}H NMR (300MHz, $CDCl_3$): δ (ppm) 1.78 (s, 12H), 2.57 (s, 12H); IR (KBr, cm^{-1}): 2919, 2850, 1450, 1431, 1310;
Elemental analysis: Calcd. for $C_{18}H_{24}$: C, 89.94; H, 10.06. Found: C, 89.91; H, 10.08.

1,4,5,8,9,12-Hexabromododecahydrotriphenylene (7)

A solution of dodecahydrotriphenylene (12.0 g, 50 mmol) in 250 mL of dry CCl_4 was added into a 500 mL round-bottomed, three-necked flask fitted with an addition funnel and a condenser. The reaction flask was cooled in an ice-water bath and the reaction mixture was stirred and illuminated with a 300 W incandescent bulb. A solution of 50 g (313 mmol) of liquid bromine in 80 mL of dry CCl_4 was added in a dropwise way over a period of about 30–40 min. Then the reaction mixture was stirred and illuminated at room temperature for an additional 30 min, and gently refluxed 0.5 h. After traces of bromine and HBr were removed by bubbling nitrogen into the resulting suspension, the precipitation was collected by filtration, washed with ethanol and dried in vacuum to yield 18.3 g of whitish powder. The filtrate was condensed under reduced pressure to afford another 12.8 g whitish powder. The combination of the two whitish powder resulted in 31.3 g total amount of the product in 87 % yield. In three similar experiments the yields were 85, 86, and 87%.

The whitish powder was recrystallized with petroleum ether (90–120)/ ethyl acetate to afford a colorless plate crystal. When heated to 105 °C, the product was decomposed to afford triphenylene as a colorless crystal.

^{1}H NMR (300 MHz, CDCl$_3$): δ (ppm) 6.13 (m, 6 H), 2.75 (d, J = 21 Hz, 6 H), 2.46 (d, J = 9.0 Hz, 6H);

^{13}C NMR (75.45 MHz, CDCl$_3$): δ (ppm) 28.26, 46.30, 136.48.

IR (KBr, cm^{-1}): 2908.99, 2844.77, 1631.87, 1432.47, 1343.71, 922.42, 956.86, 754.95, 714.44.

Elemental analysis: Calcd. for C$_{18}$H$_{18}$Br$_6$: C, 30.29; H, 2.54. Found: C, 30.17; H, 2.26.

Pentathiotriphenylene (8)

3.57 g (5.0 mmol) of 1,4,5,8,9,12-hexabromododecahydrotriphenylene was suspended in a mixture of 20 mL of DMSO and 5 mL of DMF in a 50 mL round-bottomed flask. Then an excess of Na$_2$S·9H$_2$O (5.4 g, 22.5 mmol) in 5 mL of water was added and allowed to stir for 10 h at room temperature. Cold water (160 mL) was added into the reaction mixture and the product was precipitated out of the solution as a yellow solid. The precipitation was filtered off, washed with water and ethanol (3 × 5 mL) and dried in vacuum to yield a yellow powder 1.95 g in 98.7 % yield with a melting point greater than 300 °C. The crude product is insoluble in common solvents, even in DMSO or DMI.

IR (KBr, cm^{-1}) : 3742.57, 3421.14, 2929.97, 1667.30, 1533.84, 1440.58, 1392.96, 1094.67, 1.19.69, 951.65, 757.63, 659.30, 555.07.

The crude product (1.15 g) and DDQ (5.95 g, 26 mmol) were suspended in 20 mL of chlorobenzene and refluxed for 24 h while stirring, and then allowed to cool to room temperature. The reaction mixture was washed with aqueous Na$_2$SO$_3$ solution to remove the excess DDQ and any insoluble impurities. The organic layer was separated from the aqueous layer and dried with Na$_2$SO$_4$. The solid was filtered off and the filtrate was concentrated under reduced pressure to afford a residue, which was purified by chromatography on silica gel using petroleum ether as elutent to give **8** as a yellow powder in 20% yield. Recrystallization of **8** with ethyl acetate/ hexane gave a yellow crystal. m.p. > 300 ^{o}C .

MS (m/e): 381.9 (M$^+$);

^{1}H NMR (300MHz, CDCl$_3$): δ (ppm) 7.26(s, 2H), 7.50(d, J = 9.0Hz, 2H), 8.17(d, J = 9.0Hz, 2H);

IR (KBr, cm^{-1}): 2923.05, 1644.80, 1547.88, 1415.52, 1338.24, 1147.92, 809.59, 736.47, 669.99, 539.88.

Elemental analysis: Calcd. for C$_{18}$H$_6$S$_5$: C, 56.51; H, 1.58; S, 41.91. Found: C, 56.17; H, 1.62; S, 42.21.

3. The B3LYP/6-31G* computational analyses of 7.

3.1 Optimized geometry of 7 at B3LYP/6-31G* level and relative energy of *all-trans* and *di-trans* isomers

B3LYP/6-31G* computational analyses show that the *all-trans* configuration is the most stable one with a relative energy of 39.6 kJ · mol^{-1} lower as compared with a possible *di-trans* isomer (**Figure 1S**).

di-trans	*all-trans*
-16127.05841 au	-16127.07345 au

Relative E: 0.01504 au (39.6 kJ · mol^{-1})   0
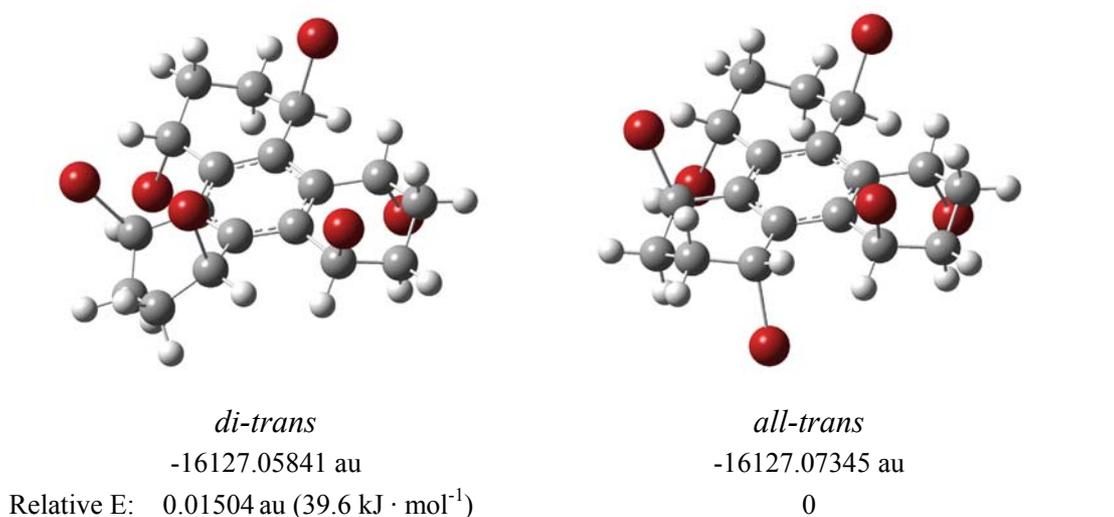
Figure 1S. Optimized geometry of 7 at B3LYP/6-31G* level and relative energy of *all-trans* and *di-trans* isomers

The above results were further supported by B3LYP/6-31G* computational analyses of four dibromo intermediates with two adjoining benzyl bromine atoms.

trans 0.0   *cis* 47.3   *trans* 3.9   *cis* 25.1 kJ mol^{-1}
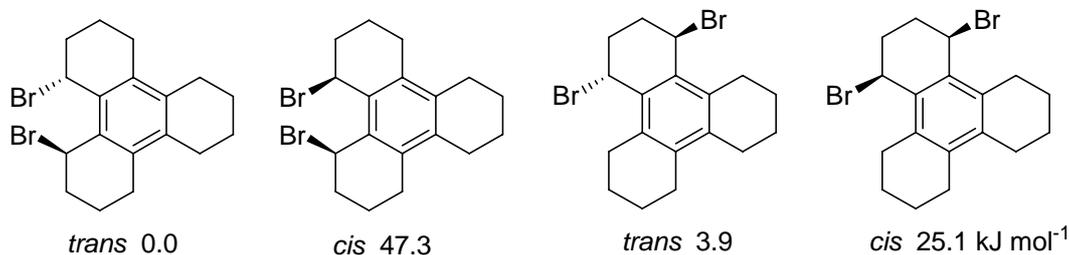
Scheme 1S. The relative energy of the four intermediates

3.2 The possible mechanism of the formation of *all-trans* isomer

The stereochemical outcome indicates that the bromination of dodecahydrotriphenylene **6** was highly stereoselective and exclusively gave *all-trans*-1,4,5,8,9,12-hexabromododecahydrotriphenylene **7**. The high stereoselectivity could be explained by the assumption that undesired isomers, i.e., a *di-trans* isomer, formed by the random collision of bromine atoms, would transfer into the *all-trans* isomer via a mechanism of the reversible free radical substitution, wherein a *cis* bromine-carbon bond in the *di-trans* isomer is broken and the central carbon atom possesses a sp^2 hybridization with a perpendicular *p* orbital. The bromine atom then would have to overlap with another lobe of *p* orbital from the less hindered side, giving the *trans* stereochemistry.

two-trans 39.6 kJ mol^{-1} all-trans 0
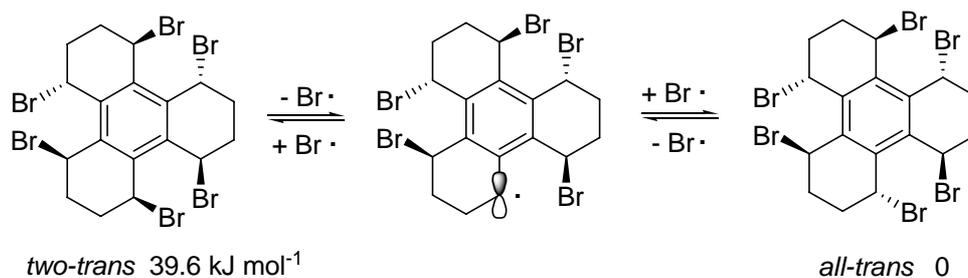
Preliminary experiments show that the *all-trans* isomer 7 is rather different in reactivity from common benzyl bromides. It was found to decompose at 105 °C, affording triphenylene as colorless needles crystals, which was proved by melting point of 200 °C [1], ^{1}H NMR and IR spectra. This indicates that **7** undergo the pyrolytic elimination at rather lower temperature compared with general alkyl bromides, which usually undergo pyrolytic elimination at above 300 °C [2]. In other words, the C–Br cleavage occurs easily in the hexabromo molecule. The reason probably results from the large molecular tension and the formation of more stable benzene rings.

[1] E. Bergmann, and O. Blum-Bergmann. *J. Am. Chem. Soc.*, **1937**, *59* (8), 1441-1442.

[2] For example, see: (a) Barton, D. H. R.; Howlett, K. E. *J. Chem. Soc.* **1949**, 155, 165-169; (b) Kampmeier, J. A.; Geer, R. P.; Meskin, A. J.; D'Silva, R. M. *J. Am. Chem. Soc.* **1966,** *88*, 1257-1265; (c) Kochi, J. K.; Singleton, D. M.; Andrews, L. J. *Tetrahedron* **1968**, *24*, 3503-3515; (d) Boothe, T. E.; Greene Jr., J. L.; Shevlin, P. B. *J. Org. Chem.* **1980**, *45*, 794-797; (e) Stark, T. J.; Nelson, N. T.; Jensen, F. R. *J. Org. Chem.* **1980**, *45*, 420-428.

4. Copies of IR, ^{1}H NMR, ^{13}C NMR, and MS spectra.
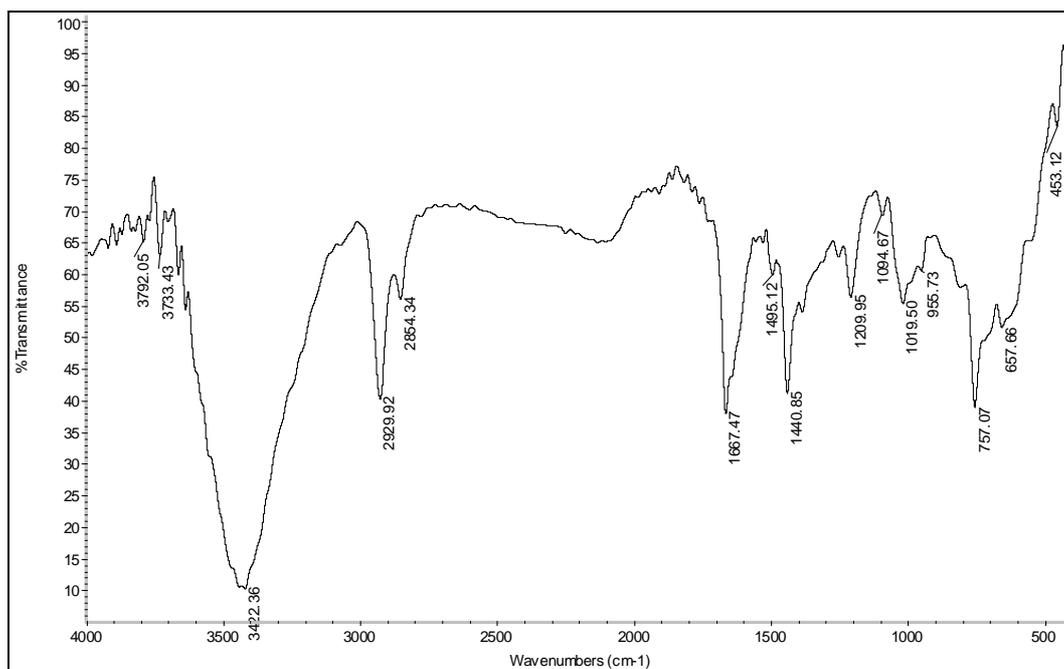
Figure 2S. The unhydrogenation intermediate product
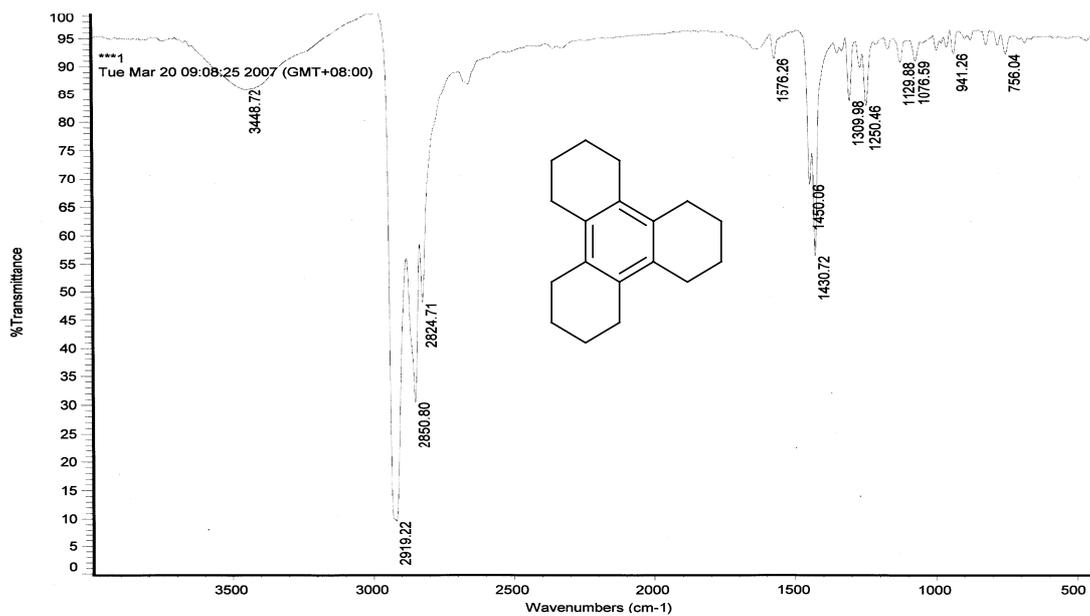
Figure 3S.   IR spectrum of compound 6.
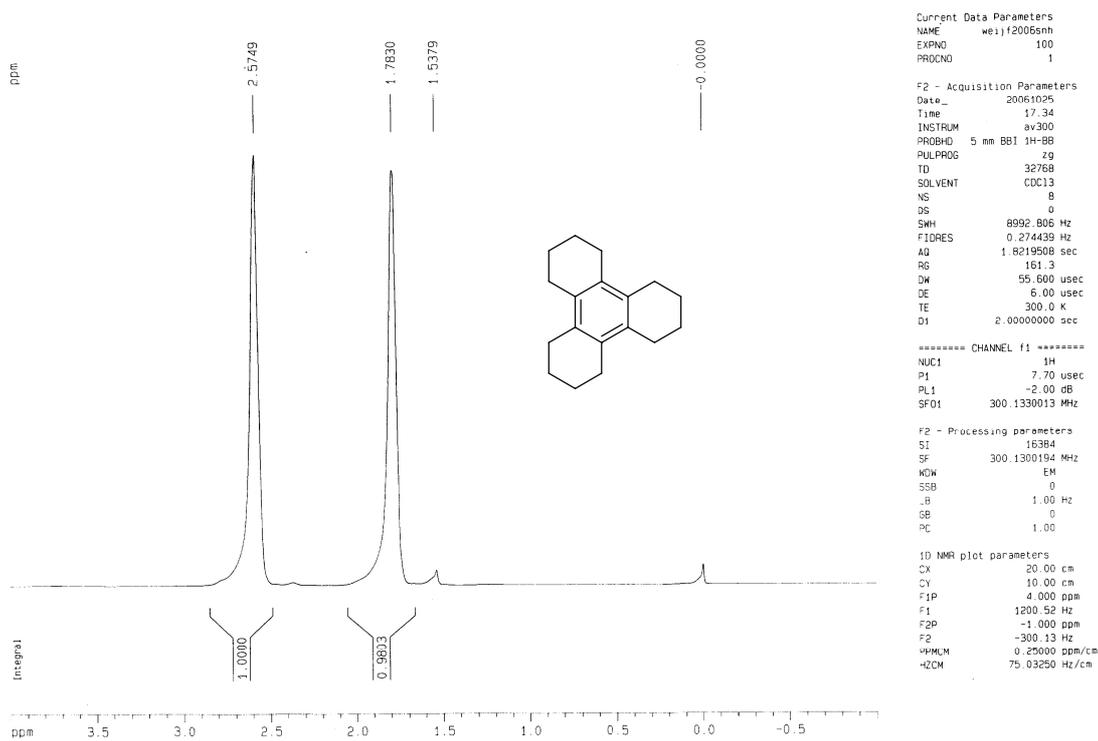
Figure 4S. ^{1}H NMR spectrum of compound 6.

6
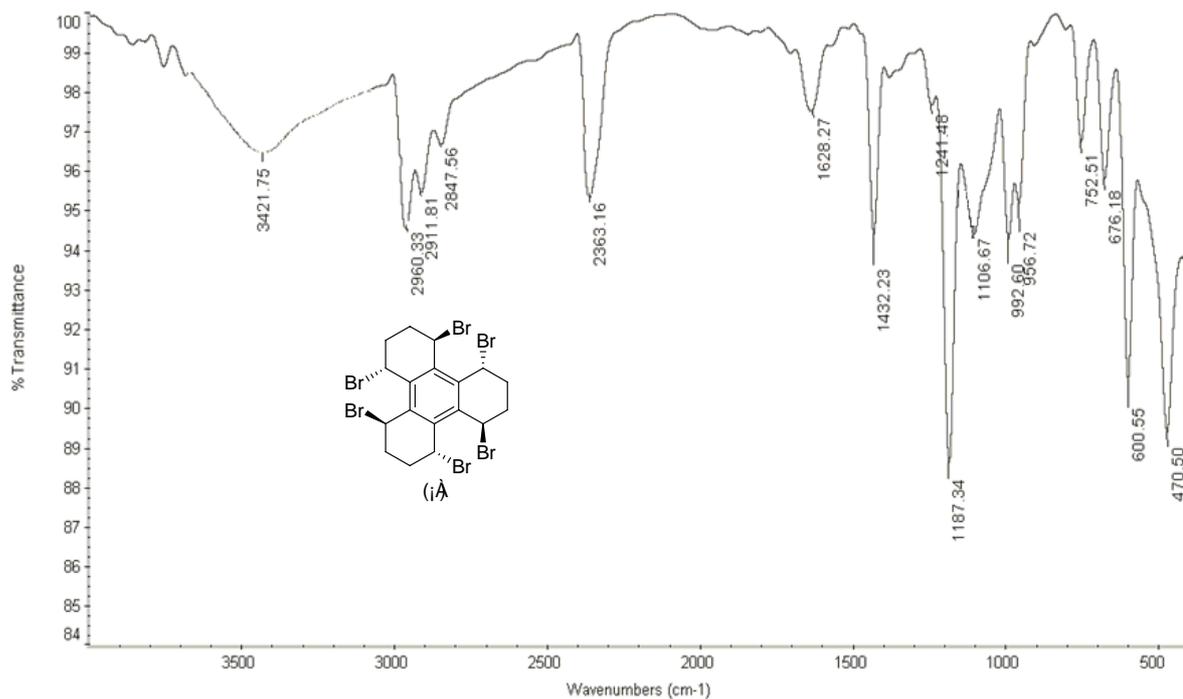
Figure 5S. IR **spectrum of compound 7.**
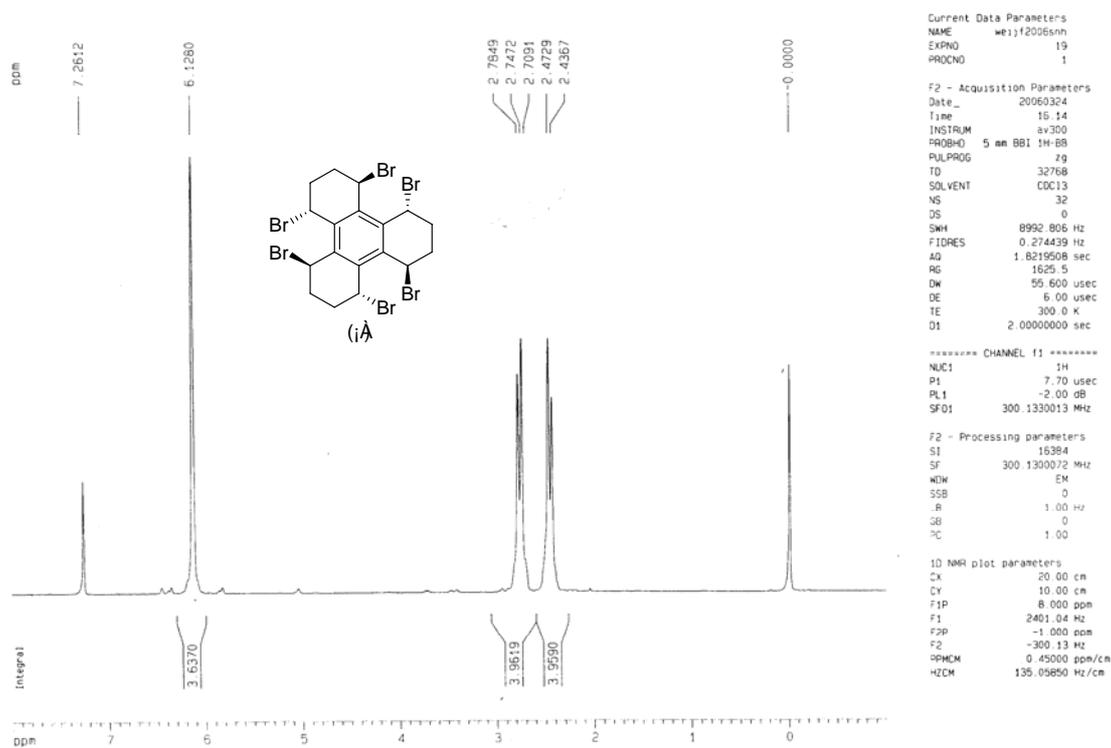
Figure 6S. ^{1}H NMR **spectrum of compound 7.**

Figure 7S. ^{13}C NMR spectrum of compound 7.

Figure 8S. ^{1}H NMR spectrum of compound 8.
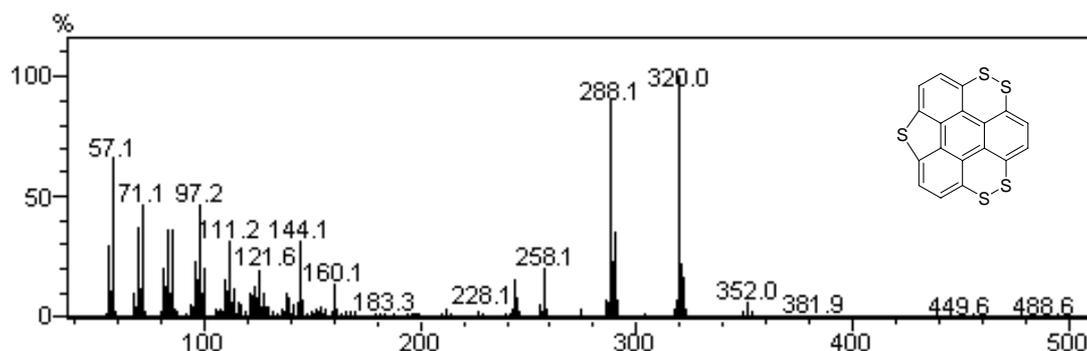
Figure 9S. MS spectrum of compound 8.

$C_{18}H_6S_5$: *m/z*, 381.9(M^+); 320.0 (100%) should be the fragment that lost two sulfur atoms, and then get a structure which molecular weight is 288.1.
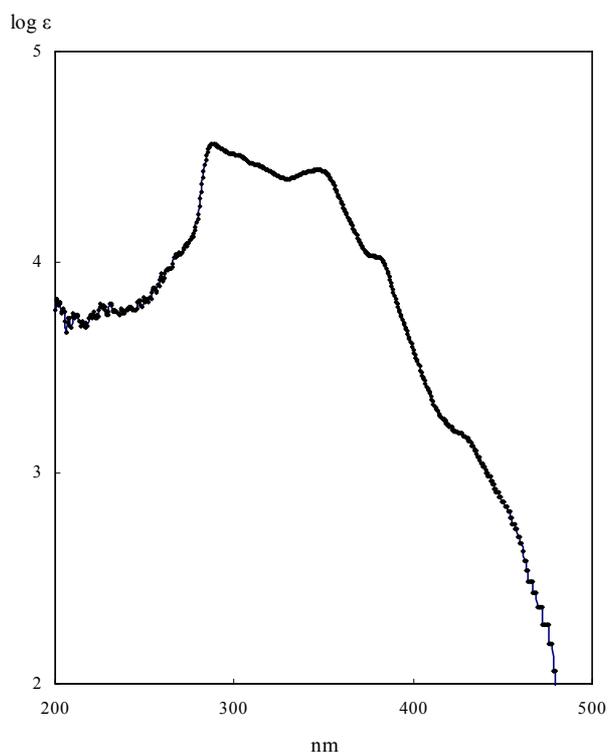
Figure 10S. Uv-vis absorption spectrum of 8 (1 mg of 8 in 100 mL of CH_2Cl_2).

5. Crystal structure determination of 7 and 8

Data for both compounds were measured on a Bruker SMART diffractometer with graphite monochromated Mo-Kα radiation (λ = 0.71073 Å) using 0.3° width steps accumulating area detector frames spanning a hemisphere of reciprocal space for both structures; the reflections were corrected for Lorentz and polarisation effects. Absorption effects were corrected on the basis of multiple equivalent reflections.

The structures were solved by direct methods and refined by full matrix least squares on F^2 using the program SHELXTL. All hydrogen atoms were included in calculated positions using a riding model. All non-hydrogen atoms were refined as anisotropic.

Crystal data for compound 7: $C_{18}H_{18}Br_6$. M = 713.78, Tetragonal, space group $I4_1/a$, $a = b = 10.724(2)$ Å, $c = 36.099(14)$ Å, $V = 4151(2)$ Å^3, T = 296(2) K, $Z = 8$, μ (Mo-Kα) = 0.71073 Å, colorless square-plate crystal, crystal dimensions 0.25 mm × 0.20 mm × 0.09 mm, crystal density 2.284 mg/m^3.

Full matrix least-squares based on F^2, gave $R_1 = 0.0413$ and w$R_2 = 0.0926$ for 1849 ($I \geq 2\sigma(I)$), GOF = 1.012 for 110 parameters.

B3LYP/3-31g* calculated structure of **7** is in agreement with that determined by X-ray crystallography, as shown in Figure 11S and 12S.
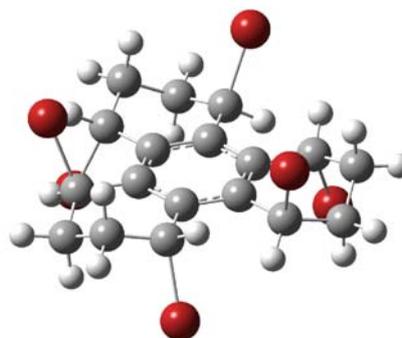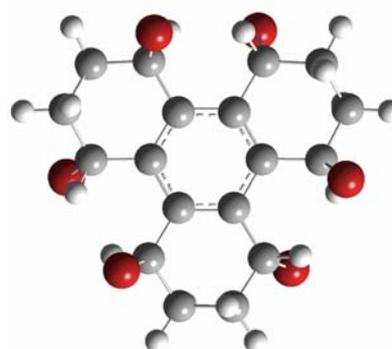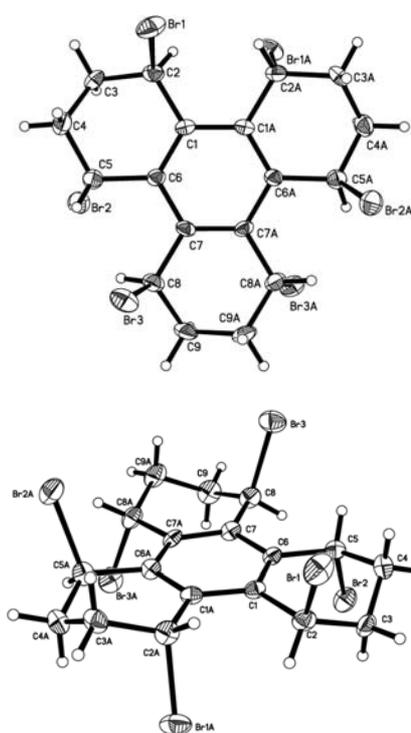
Figure 11S. Crystal structure of 7 (thermal ellipsoids: 30% probability).

Figure 12S. The B3LYP/6-31G* calculated structure of 7.

Table 1S   Bond Lengths and Bond Angles of 7.[a]

Br(1)-C(2)	1.999(7)	[2.017]	Br(2)-C(5)	2.014(7)	[2.017]
Br(3)-C(8)	2.015(7)	[2.017]	C(1)-C(2)	1.512(8)	[1.516]
C(3)-C(4)	1.507(9)	[1.530]	C(4)-C(5)	1.525(9)	[1.526]
C(1)-C(6)	1.402(8)	[1.402]	C(1)-C(1A)	1.415(12)	[1.420]
C(2)-C(3)	1.512(9)	[1.526]	C(2)-H(2)	0.9800	[1.088]
C(5)-C(6)	1.513(9)	[1.516]	C(7)-C(7A)	1.394(12)	[1.402]
C(8)-H(8)	0.9800	[1.088]	C(9)-H(9B)	0.9700	[1.098]
C(3)-H(3A)	0.9700	[1.092]	C(3)-H(3B)	0.9700	[1.098]
C(4)-H(4A)	0.9700	[1.092]	C(4)-H(4B)	0.9700	[1.098]

C(5)-H(5)	0.9800	[1.088]	C(6)-C(7)	1.422(8)	[1.420]
C(7)-C(8)	1.513(8)	[1.516]	C(8)-C(9)	1.507(9)	[1.526]
C(9)-H(9A)	0.9700	[1.092]	C(9)-C(9A)	1.518(14)	[1.530]
C(6)-C(1)-C(1A)	119.7(3)		C(6)-C(1)-C(2)	119.9(6)	
C(1A)-C(1)-C(2)	120.4(4)		C(1)-C(2)-Br(1)	109.6(4)	
C(3)-C(2)-C(1)	114.8(5)		C(3)-C(2)-Br(1)	107.2(5)	
Br(1)-C(2)-H(2)	108.3		C(2)-C(3)-H(3A)	109.3	
C(3)-C(2)-H(2)	108.3		C(1)-C(2)-H(2)	108.3	
C(4)-C(3)-C(2)	111.5(5)		C(4)-C(3)-H(3A)	109.3	
H(3A)-C(3)-H(3B)	108.0		C(5)-C(4)-H(4A)	109.7	
C(4)-C(3)-H(3B)	109.3		C(2)-C(3)-H(3B)	109.3	
C(3)-C(4)-C(5)	109.8(6)		C(3)-C(4)-H(4A)	109.7	
C(3)-C(4)-H(4B)	109.7		C(5)-C(4)-H(4B)	109.7	
C(6)-C(5)-C(4)	115.5(5)		C(6)-C(5)-Br(2)	107.1(4)	
H(4A)-C(4)-H(4B)	108.2		C(4)-C(5)-Br(2)	107.7(4)	
C(6)-C(5)-H(5)	108.8		C(4)-C(5)-H(5)	108.8	
Br(2)-C(5)-H(5)	108.8		C(7)-C(6)-C(5)	118.3(5)	
C(1)-C(6)-C(7)	120.4(5)		C(1)-C(6)-C(5)	121.3(5)	
C(6)-C(7)-C(8)	119.6(5)		C(7)-C(8)-Br(3)	108.1(4)	
C(7A)-C(7)-C(6)	119.7(3)		C(7A)-C(7)-C(8)	120.6(4)	
C(9)-C(8)-C(7)	114.5(6)		C(9)-C(8)-Br(3)	108.7(5)	
H(9A)-C(9)-H(9B)	108.1		C(7)-C(8)-H(8)	108.5	
C(8)-C(9)-C(9A)	110.3(5)		C(8)-C(9)-H(9A)	109.6	
C(8)-C(9)-H(9B)	109.6		C(9)-C(8)-H(8)	108.5	
Br(3)-C(8)-H(8)	108.5		C(9A)-C(9)-H(9A)	109.6	
C(9A)-C(9)-H(9B)	109.6				

a **Calculated values in [ ]**
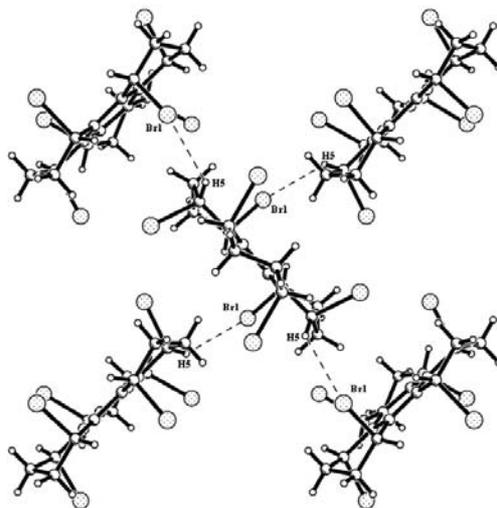
Figure 13S. The packing diagram of 7 (intermolecular H-bonds) (thermal ellipsoids: 30% probability).

Crystal data for compound 8: $C_{18}H_6S_5$: M = 382.53, Orthorhombic, space group: P_{nma}, a = 6.9134(5) Å, b = 19.5698(14) Å, c = 10.8775(8) Å, V = 1471.66(18) Å^3, T = 296(2) K, Z = 4, μ (Mo-Kα) = 0.71073 Å, block yellow crystal, crystal dimensions: 0.37 mm × 0.28 mm × 0.15 mm, crystal density: 1.726 mg/m^3.

Full matrix least-squares based on F^2, gave $R_1 = 0.0418$ and $wR_2 = 0.1207$ for 2624 ($I \geq 2\sigma$ (I)), GOF = 1.070 for 208 parameters.

B3LYP/3-31g* calculated structure of **8** is in agreement with that determined by X-ray crystallography, as shown in Figure 15S.
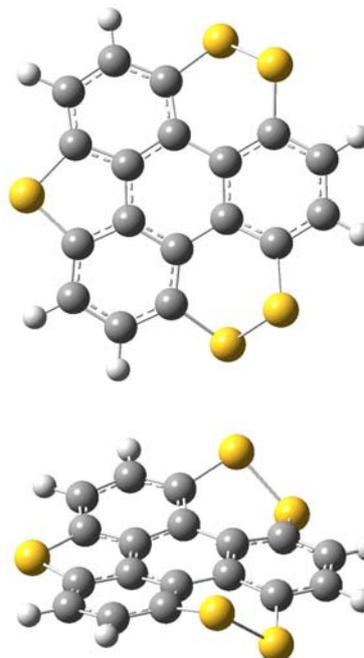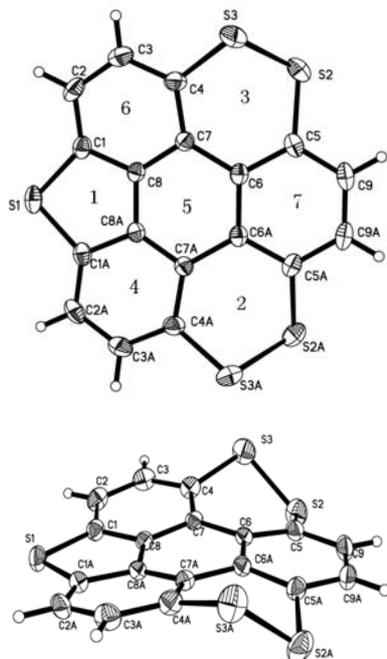
Figure 14S. Crystal structure of 8 (thermal ellipsoids: 30% probability).

Figure 15S. Optimized geometry of 8 at B3LYP/6-31G* level

Table 2S.   Bond Lengths and Bond Angles of 8. [a]

S(1)-C(8)	1.732(6)	[1.776]	C(5)-C(14)	1.455(6)	[1.471]	C(3)-C(4)	1.383(8)	[1.400]
S(1)-C(1)	1.773(6)	[1.776]	C(6)-C(7)	1.409(4)	[1.417]	C(3)-H(3)	0.9300	[1.086]
S(2)-C(4)	1.767(5)	[1.784]	C(7)-C(12)	1.348(6)	[1.403]	C(4)-C(5)	1.410(7)	[1.417]
S(2)-S(3)	2.052(3)	[2.094]	C(7)-C(8)	1.438(8)	[1.410]	C(5)-C(6)	1.434(6)	[1.403]
S(3)-C(15)	1.750(6)	[1.786]	C(8)-C(9)	1.368(7)	[1.388]	C(15)-C(16)	1.354(7)	[1.389]
S(4)-C(18)	1.774(5)	[1.786]	C(9)-C(10)	1.387(10)	[1.403]	C(14)-C(15)	1.430(6)	[1.423]
S(4)-S(5)	2.039(3)	[2.094]	C(9)-H(9)	0.9300	[1.085]	C(13)-C(14)	1.423(4)	[1.441]
S(5)-C(11)	1.757(5)	[1.784]	C(10)-C(11)	1.398(8)	[1.400]	C(17)-H(17)	0.9300	[1.086]
C(1)-C(6)	1.371(8)	[1.410]	C(10)-H(10)	0.9300	[1.086]	C(17)-C(18)	1.407(7)	[1.389]
C(1)-C(2)	1.382(7)	[1.388]	C(11)-C(12)	1.408(6)	[1.417]	C(16)-C(17)	1.384(5)	[1.394]
C(2)-C(3)	1.390(9)	[1.403]	C(12)-C(13)	1.483(6)	[1.471]	C(16)-H(16)	0.9300	[1.086]
C(2)-H(2)	0.9300	[1.085]	C(13)-C(18)	1.400(6)	[1.423]			
C(8)-S(1)-C(1)	92.01(13)		C(4)-S(2)-S(3)	97.6(2)		C(18)-S(4)-S(5)	100.5(2)	
C(11)-S(5)-S(4)	98.4(2)		C(6)-C(1)-C(2)	121.4(6)		C(6)-C(1)-S(1)	109.0(4)	
C(2)-C(1)-S(1)	128.9(5)		C(1)-C(2)-C(3)	117.0(5)		C(1)-C(2)-H(2)	121.5	
C(3)-C(2)-H(2)	121.5		C(4)-C(3)-C(2)	122.5(4)		C(4)-C(3)-H(3)	118.7	
C(2)-C(3)-H(3)	118.8		C(3)-C(4)-C(5)	121.6(5)		C(3)-C(4)-S(2)	118.7(4)	
C(5)-C(4)-S(2)	119.2(4)		C(4)-C(5)-C(6)	114.4(4)		C(4)-C(5)-C(14)	128.3(4)	
C(6)-C(5)-C(14)	117.3(4)		C(1)-C(6)-C(7)	117.4(5)		C(1)-C(6)-C(5)	122.9(5)	
C(7)-C(6)-C(5)	119.1(5)		C(12)-C(7)-C(6)	125.5(5)		C(12)-C(7)-C(8)	124.8(4)	
C(6)-C(7)-C(8)	109.4(6)		C(9)-C(8)-C(7)	116.8(6)		C(9)-C(8)-S(1)	131.2(5)	
C(7)-C(8)-S(1)	112.0(4)		C(8)-C(9)-C(10)	119.5(5)		C(8)-C(9)-H(9)	120.2	

C(10)-C(9)-H(9)	120.3	C(9)-C(10)-C(11)	122.3(4)	C(9)-C(10)-H(10)	118.8
C(11)-C(10)-H(10)	118.9	C(10)-C(11)-C(12)	119.2(5)	C(10)-C(1)-S(5)	119.7(4)
C(12)-C(1)-S(5)	120.5(4)	C(7)-C(12)-C(11)	116.9(4)	C(7)-C(12)-C(13)	116.6(4)
C(11)-C(1)-C(13)	126.4(4)	C(18)-C(13)-C(14)	118.1(4)	C(18)-C(13)-C(12)	122.3(4)
C(14)-C(1)-C(12)	119.6(4)	C(13)-C(14)-C(15)	118.8(5)	C(13)-C(1)-C(5)	120.6(4)
C(15)-C(1)-C(5)	120.0(4)	C(16)-C(15)-C(14)	121.7(5)	C(16)-C(1)-S(3)	115.0(4)
C(14)-C(1)-S(3)	122.5(4)	C(15)-C(16)-C(17)	119.7(5)	C(15)-C(16)-H(16)	120.2
C(17)-C(16)-H(16)	120.2	C(16)-C(17)-C(18)	120.6(5)	C(16)-C(17)-H(17)	119.7
C(18)-C(17)-H(17)	119.7	C(13)-C(18)-C(17)	120.8(5)	C(13)-C(1)-S(4)	120.8(3)
C(17)-C(18)-S(4)	117.7(4)	C(15)-S(3)-S(2)	99.9(2)		

^{a} **Calculated values in [ ]**
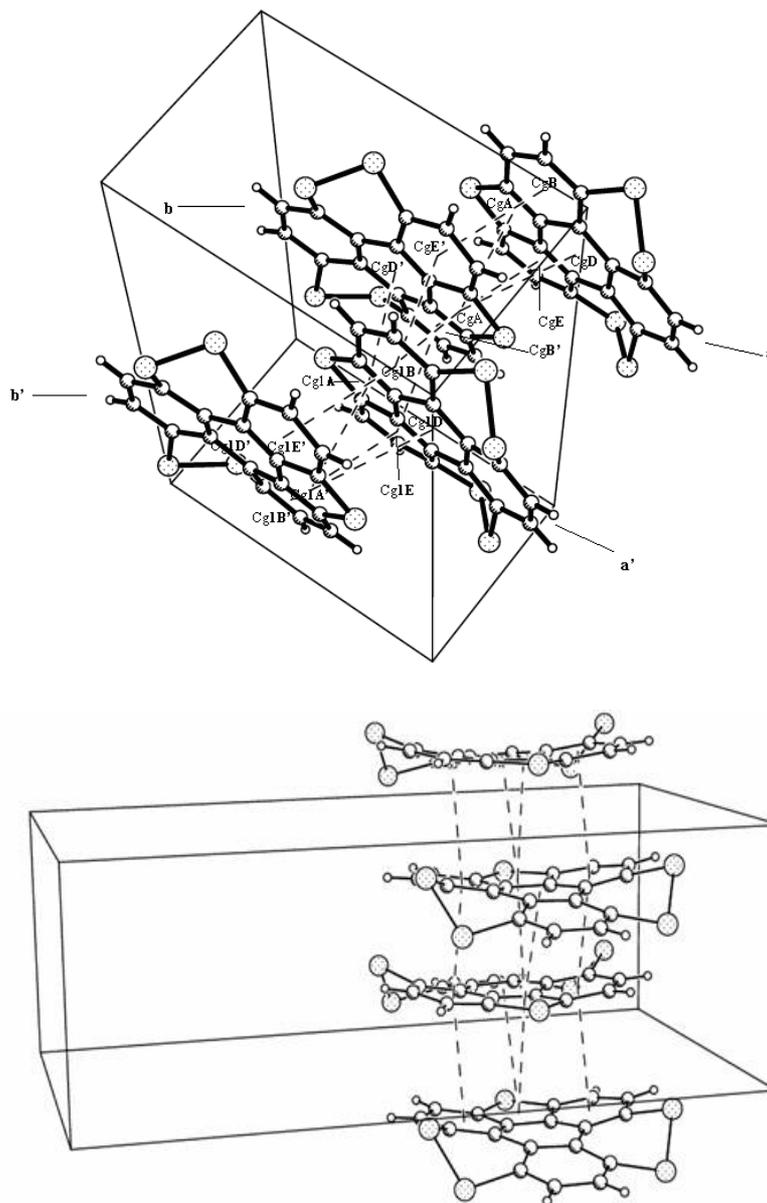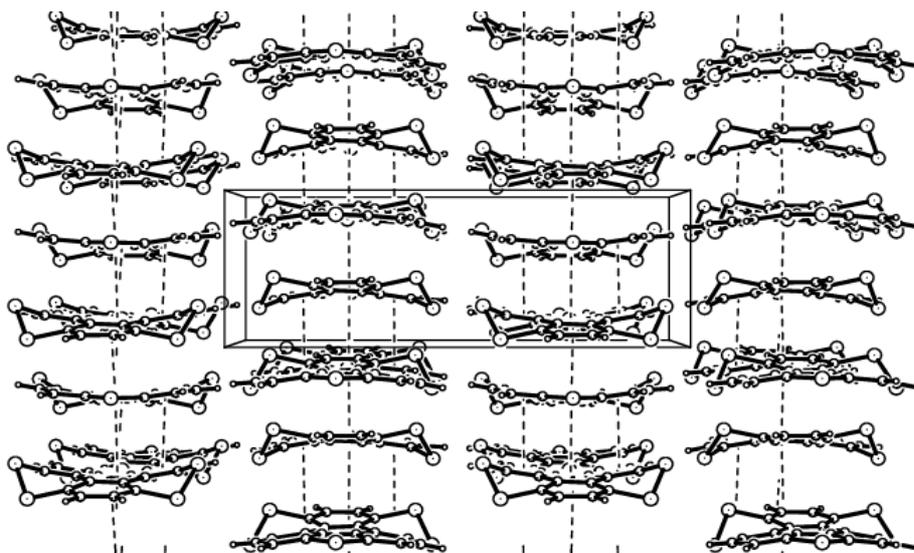
Figure 16S. Crystal packing diagram of 8 (π–π stacking interactions) (thermal ellipsoids: 30% probability).

.

The crystal packing diagram of **8** (Fig. 16S) indicates that there are π–π stacking interactions existing in the ring 1, ring 4, ring 5 and ring 6 of two neighboring molecules. Seen from Figure 12S, there are quadruple π–π stacking interactions between neighboring molecules **a** and **b**, the core-core separation is 3.518 Å, 3.752 Å, 3.640 Å, 3.626 Å, respectively. This quadruple π–π stacking interaction also exists in the molecule **a'** and **b** and the core-core separation is 3.517nm, 3.753nm, 3.640nm, 3.627nm, which is identical with that in molecular a and b.